

Net 426-Gb/s and 11.83-b/s/Hz 80-km Transmission with an Integrated SiP Dual-Polarization Direct Detection Receiver

Jingchi Li⁽¹⁾, Zhen Wang⁽¹⁾, Xingfeng Li⁽¹⁾, Haoshuo Chen⁽²⁾, William Shieh⁽³⁾, Yikai Su⁽¹⁾

⁽¹⁾ State Key Laboratory of Advanced Optical Communication Systems and Networks, Department of Electronic Engineering, Shanghai Jiao Tong University, 800 Dongchuan Rd, Shanghai, 200240, China, yikaisu@sjtu.edu.cn

⁽²⁾ Nokia Bell Labs, 600 Mountain Ave, Murray Hill, NJ 07974, USA

⁽³⁾ School of Engineering, Westlake University, Hangzhou 310030, China

Abstract We experimentally demonstrate a single-wavelength 528-Gb/s dual-polarization OFDM 16-QAM signal transmission over an 80-km SMF with a silicon photonic dual-polarization carrier-assisted differential detection receiver, which achieves the record 426-Gb/s net data rate and 11.83-b/s/Hz net ESE for an integrated direct detection receiver. ©2023 The Author(s)

Introduction

The ever-increasing data traffic demand driven by emerging applications has propelled the optical communications research towards higher data rates. For short-reach interconnect scenarios, an important consideration is to maintain a low cost, which can be addressed by introducing emerging photonic integration techniques [1-2]. Low-cost and compact photonic integrated transceivers beyond 400G play a significant role for future 800 GE or 1.6 TbE.

Compared to a direct detection (DD) receiver, a coherent receiver exhibits a higher capacity and better tolerance to optical impairments, originating from its field recovery capability relying on a narrow-linewidth local oscillator (LO). By leveraging the photonic integration techniques, the footprint and power consumption of a coherent receiver has been dramatically reduced, which opens the door for its application in cost-sensitive short-reach scenarios. However, the fabrication of the narrow-linewidth integrated laser remains the key challenge for a monolithic integrated coherent receiver due to the material incompatibility. Additionally, the precise wavelength alignment between transceiver lasers increases the implementation cost. Consequently, integrated LO-free DD receivers have drawn tremendous interest in cost-effective short reach scenarios. As a conventional DD receiver offers limited sensitivity and electrical spectral efficiency (ESE), a variety of advanced DD schemes have been demonstrated to improve the overall performance of the DD. In [3-4], a silicon photonic (SiP) carrier-assisted differential detection (CADD) receiver was fabricated to achieve the transmission of net 182-Gb/s over 80-km single-mode fiber (SMF) with a net ESE of 5.2-b/s/Hz. In [5], net 258-Gb/s and net 5.31-b/s/Hz ESE transmission over 40-km SMF was presented using a SiP phase diversity

receiver. To satisfy the growing capacity demand like beyond 400G/λ, it is highly desirable to take advantage of polarization diversity in a similar manner to high-rate coherent technology, and explore the four-dimension (intensity and phase in dual polarization) integrated dual-polarization (DP) DD receivers.

In this paper, we demonstrate beyond 400G transmission using an integrated SiP DP-CADD receiver, which is the first on-chip DD receiver with field recovery capability of a four-dimensional complex-valued DSB signal, as a DP-coherent receiver does. A low-cost automated silicon polarization controller (ASPC) is implemented for polarization tracking, followed by two single-polarization CADD receivers for signal reception. The DP complex-valued DSB signal can be successfully detected without needing for an LO which is indispensable in a coherent receiver. In the experiment, a 528-Gb/s OFDM 16-QAM signal with a 36-GHz electrical bandwidth is successfully transmitted over 80-km SMF. Considering the 24% SD-FEC threshold [6], the net data rate and net ESE are 426 Gb/s and 11.83 b/s/Hz, respectively. Fig. 1 summarizes the recent progresses for integrated DD receivers [3-5, 7-11]. To our best knowledge, we achieve the highest capacity and ESE for an integrated DD receiver.

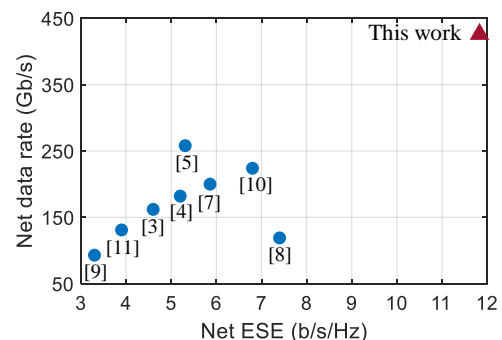


Fig. 1: Recent progresses for integrated DD receivers.

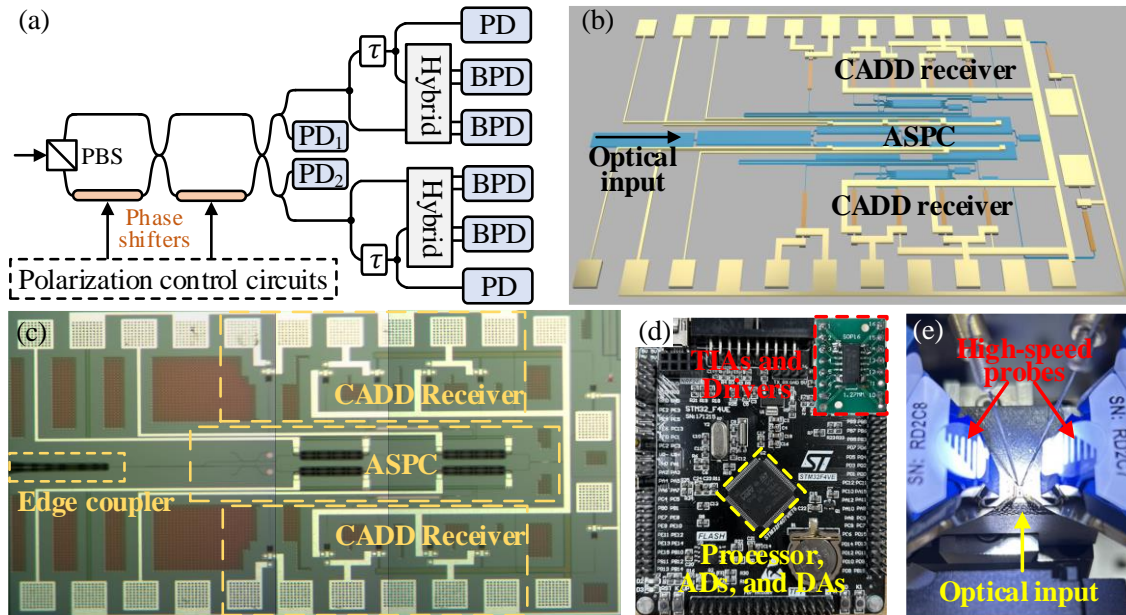


Fig. 2: (a) Schematic of the DP-CADD receiver. (b) 3-D illustration of the integrated DP-CADD receiver. (c) Optical microscopy image of the fabricated integrated DP-CADD receiver. (d) Polarization control circuits. (e) Test platform.

DP-CADD Receiver Design and Fabrication

Fig. 2(a) presents the schematic of the DP-CADD receiver, with the 3-D illustration of the integrated DP-CADD receiver given in Fig. 2(b). Since the state of polarization of the DP-signal varies randomly during fiber transmission, the carrier may suffer from the polarization fading issue [12]. Therefore, an ASPC is implemented to adjust the polarization automatically. The ASPC consists of the integrated polarization tuning units [13] and off-chip control circuits shown in Fig. 2(d). Firstly, the input light is separated into TE and TM portions using a polarization splitter and rotator (PSR), with the TM portion rotated to the TE light simultaneously. Then, a balanced Mach-Zehnder interferometer (MZI) is applied to split the signal into two polarizations with equal power at its output, which is realized by tuning the thermal phase shifters automatically using the off-chip control circuits. Finally, the outputs of the ASPC are detected with two integrated single-polarization CADD receivers, which consist of

optical couplers, optical delay lines, 90-degree optical hybrids and several photodiodes (PDs) [14]. Fig.2 (c) gives the optical microscopy image of the fabricated SiP DP-CADD receiver with a footprint of $\sim 1.8 \text{ mm} \times 1.0 \text{ mm}$. An edge coupler with $\sim 4 \text{ dB/facet}$ insertion loss is used to couple the random polarized light into the chip. We design the optical delay as 23 ps. The on-chip PD, with a 38-GHz 6-dB bandwidth at -2 V bias, was biased at -4 V for high-capacity transmission. Fig. 2(e) shows the test platform of the silicon chip. The devices were fabricated on a 220-nm commercial silicon-on-insulator (SOI) wafer with a standard CMOS manufacturing process.

Experimental Setup and DSP flow charts

Fig. 3 shows the experimental setup and DSP flow charts. At the transmitter side, a 15-kHz external cavity laser (ECL) is used as the light source, and the 528-Gb/s OFDM 16-QAM signal is generated with a 100-GSa/s digital-to-analog converter (DAC) (Micram DAC4). The modulated carrier-suppressed optical signal enters a

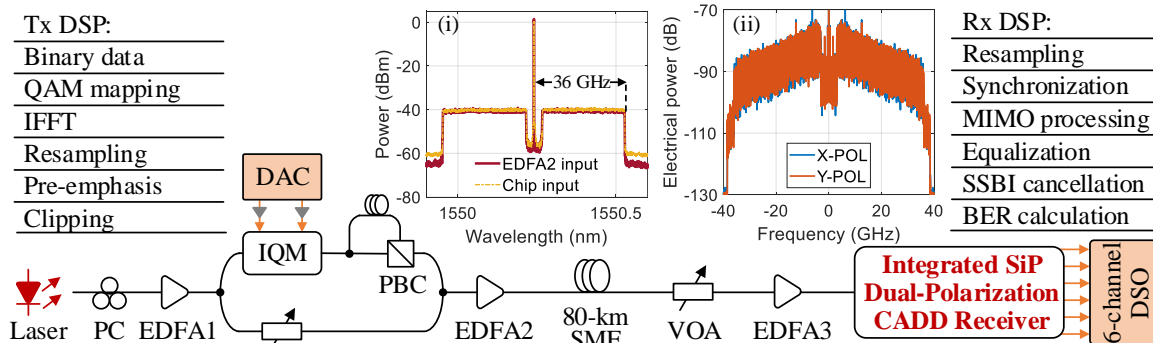


Fig. 3: Experimental setup and DSP flow charts of 528-Gb/s transmission based on SiP DP-CADD receiver. Insets: (i) measured optical spectra in the transmission case, (ii) Electrical spectra detected with single-ended PD.

polarization emulator, which consists of the optical couplers, optical delay line, and polarization beam combiner. Then, an optical coupler is used to combine the DP-signal with the carrier. After being amplified by an erbium-doped fiber amplifier (EDFA), the carrier-assisted DP-signal is launched into an 80-km fiber link. At the receiver side, another EDFA is used to amplify the signal, which is then coupled into the silicon chip and detected with the SiP DP-CADD receiver. The inset (i) plots the optical spectra in the transmission case. The electrical bandwidth of the 528-Gb/s signal is 36 GHz, with a 3-GHz guard band inserted between the carrier and sideband to combat the severe signal-signal beat interference (SSBI) enhancement [14]. The electrical spectra detected with single-ended PD of X and Y polarizations are shown in the inset (ii), respectively. Finally, the detected photocurrents are sampled by an 80-GSa/s digital storage oscilloscope (DSO) (LeCroy 36Zi-A). The transceiver DSP algorithms are also provided in Fig. 3. The transmitter DSP includes pre-emphasis and peak-to-average-power ratio clipping. At the receiver, MIMO processing of two polarization signals is used for polarization demultiplexing. Then, equalization, single-stage SSBI cancellation, and BER calculation are employed in each polarization.

Results and Discussion

We firstly verify the feasibility of the ASPC in the experiment. Fig. 4 demonstrates the automated polarization tuning progress. The voltages are obtained based on the photocurrents detected by monitored PD₁ and PD₂ in Fig. 2(a). When the ASPC is disabled, the random polarization shift causes significant power difference between two polarizations, leading to a channel singularity. After the ASPC is switched on, equal optical power at two outputs can be obtained, and the signals of both polarizations are successfully recovered as shown. Note that the burr of waveform is mainly caused by the circuit noise which can be reduced with circuit optimization.

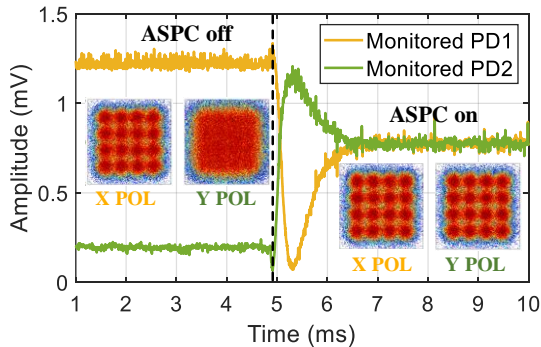


Fig. 4: On-chip automated polarization tuning progress and the recovered constellations in different states.

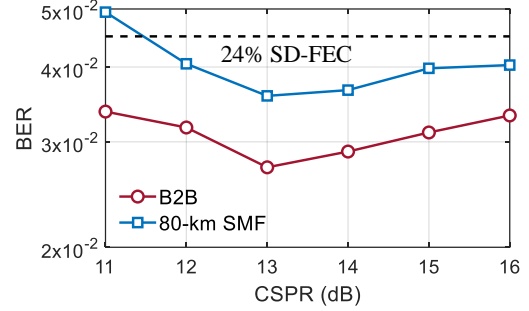


Fig. 5: BER vs. CSRP in both B2B and transmission cases.

Fig. 5 presents the BER results at different CSRP conditions. As shown, in the back-to-back (B2B) and 80-km SMF transmission cases, the optimal CSRPs are both 13 dB, which is a trade-off between the linear beating term and effective signal powers. Finally, we measure the receiver sensitivity by varying the variable optical attenuator (VOA) at the receiver in two cases. It can be observed in Fig. 6 that the BER of 528-Gb/s OFDM 16-QAM signal after 80-km SMF transmission is below the 24% SD-FEC threshold of 4.5×10^{-2} [6]. The insets (i-iv) illustrate the recovered constellations of X and Y polarizations at -9 -dB ROP in the B2B case and transmission cases, respectively.

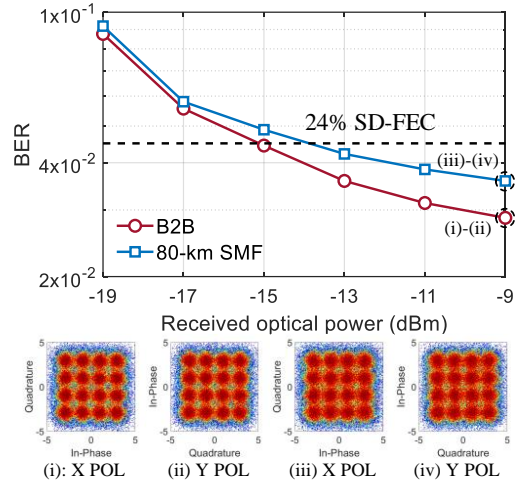


Fig. 6: ROP sensitivity curves measured in both B2B and transmission cases. Insets (i-iv): recovered constellations of X and Y polarizations at -9 -dB ROP in two cases.

Conclusions

In conclusion, we have demonstrated an integrated SiP DP-CADD receiver. A 528-Gb/s OFDM 16-QAM signal is successfully recovered after transmitted over 80-km SMF, achieving the highest 426-Gb/ net data rate and the highest 11.83-b/s/Hz net ESE for an integrated DD receiver, to the best of our knowledge. We believe that the demonstration of the high-capacity and high-ESE LO-free integrated receiver provides a promising low-cost solution for next-generation data center interconnects and short-reach communications.

References

- [1] Mathieu Chagnon, "Optical Communications for Short Reach," *Journal of Lightwave Technology*, vol. 37, no. 8, pp. 1779–1797, 2023. DOI: [10.1109/JLT.2019.2901201](https://doi.org/10.1109/JLT.2019.2901201)
- [2] Wei Shi, Ye Tian, and Antoine Gervais, "Scaling capacity of fiber-optic transmission systems via silicon photonics," *Nanophotonics*, vol. 9, no. 16, pp. 4629–4663, 2020. DOI: [10.1515/nanoph-2020-0309](https://doi.org/10.1515/nanoph-2020-0309)
- [3] Jingchi Li, Zhen Wang, Honglin Ji, Xingfeng Li, Haoshuo Chen, Ranjith Rajasekharan Unnithan, William Shieh, and Yikai Su, "High Electrical Spectral Efficiency Silicon Photonic Receiver with Carrier-Assisted Differential Detection," in *Optical Fiber Communication Conference (OFC)*, San Diego, California United States, 2022, Paper Th4B. 6. DOI: [10.1364/OFC.2022.Th4B.6](https://doi.org/10.1364/OFC.2022.Th4B.6)
- [4] Jingchi Li, Zhen Wang, Honglin Ji, Xingfeng Li, Haoshuo Chen, Ranjith Rajasekharan Unnithan, William Shieh, and Yikai Su, "Silicon Photonic Carrier-Assisted Differential Detection Receiver With High Electrical Spectral Efficiency for Short-Reach Interconnects," *Journal of Lightwave Technology*, vol. 41, no. 3, pp. 919–925, 2023. DOI: [10.1109/JLT.2022.3211308](https://doi.org/10.1109/JLT.2022.3211308)
- [5] Yixiang Hu, Xueyang Li, Deng Mao, Md Samiul Alam, Essam Berikaa, Jinsong Zhang, Santiago Bernal, Alireza Samani, Mohammad E. Mousa-Pasandi, Maurice O'Sullivan, and David V. Plant, "Silicon Photonic Phase-diverse Receiver Enabling Transmission of >Net 250 Gbps/λ over 40 km for High-speed and Low-cost Short-Reach Optical Communications," *Journal of Lightwave Technology*, 2023, DOI: [10.1109/JLT.2023.3271672](https://doi.org/10.1109/JLT.2023.3271672)
- [6] Fred Buchali, Axel Klekamp, Laurent Schmalen, and Tomislav Drenski, "Implementation of 64QAM at 42.66 GBaud Using 1.5 Samples per Symbol DAC and Demonstration of up to 300 km Fiber Transmission," in *Optical Fiber Communication Conference (OFC)*, San Francisco, California United States, 2014, Paper M2A.1. DOI: [10.1364/OFC.2014.M2A.1](https://doi.org/10.1364/OFC.2014.M2A.1)
- [7] Yixiang Hu, Xueyang Li, Deng Mao, Md Samiul Alam, Essam Berikaa, Jinsong Zhang, Alireza Samani, Mohammad E. Mousa-Pasandi, Maurice O'Sullivan, Charles Laperle, and David V. Plant, "Transmission of Net 200 Gbps/λ over 40 km of SMF Using an Integrated SiP Phase-Diverse Receiver," in Proc. *European Conference on Optical Communication (ECOC)*, Basel, Switzerland, 2022, Paper Th3B.6.
- [8] Po Dong, Xi Chen, Kwangwoong Kim, S. Chandrasekhar, Young-Kai Chen, and Jeffrey H. Sinsky, "128-Gb/s 100-km transmission with direct detection using silicon photonic Stokes vector receiver and I/Q modulator," *Optics Express*, vol. 24, no 13, pp. 14208–14214, 2016. DOI: [10.1364/OE.24.014208](https://doi.org/10.1364/OE.24.014208)
- [9] Yeyu Tong, Qiulin Zhang, Xinru Wu, Chester Shu, and Hon Ki Tsang, "112 Gb/s 16-QAM OFDM for 80-km data center interconnects using silicon Photonic integrated circuits and Kramers–Kronig detection," *Journal of Lightwave Technology*, vol. 37, no. 14, pp. 3532–3538, 2019. DOI: [10.1109/JLT.2019.2917614](https://doi.org/10.1109/JLT.2019.2917614)
- [10] Sen Zhang, Liwang Lu, Linsheng Fan, Bin Chen, Tingting Zhang, Tianjian Zuo, Lei Liu, Jin Tang, Li Zeng, Pengxin Chen, Jiahao Huo, Xian Zhou, Alan Pak Tao Lau, Chao Lu, Liu Liu, and Changjian Guo, "224-Gb/s 16QAM SV-DD Transmission Using Pilot-Assisted Polarization Recovery with Integrated Receiver," in *Optical Fiber Communication Conference (OFC)*, Washington, DC United States, 2021. DOI: [10.1364/OFC.2021.W7F.4](https://doi.org/10.1364/OFC.2021.W7F.4)
- [11] Yang Hong, Ke Li, Cosimo Lacava, Shenghao Liu, David J. Thomson, Fanfan Meng, Xiaoke Ruan, Fan Zhang, Graham T. Reed, and Periklis Petropoulos, "High-Speed DD Transmission Using a Silicon Receiver Co-Integrated With a 28-nm CMOS Gain-Tunable Fully-Differential TIA," *Journal of Lightwave Technology*, vol. 39, no. 4, pp. 1138–1147, 2021. DOI: [10.1109/JLT.2020.3028221](https://doi.org/10.1109/JLT.2020.3028221)
- [12] Di Che, Chuan Bowen Sun, and William Shieh, "Direct detection of the optical field beyond single polarization mode," *Optics Express*, vol. 26, no. 3, pp. 3368–3380, 2018. DOI: [10.1364/OE.26.003368](https://doi.org/10.1364/OE.26.003368)
- [13] Minglei Ma, Kyle Murray, Mengyuan Ye, Stephen Lin, Yun Wang, Zeqin Lu, Han Yun, Ricky Hu, Nicolas A. F. Jaeger, and Lukas Chrostowski, "Silicon Photonic Polarization Receiver with Automated Stabilization for Arbitrary Input Polarizations," in *Conference on Lasers and Electro-Optics (CLEO)*, San Jose, California United States, 2016, Paper STu4G.8. DOI: [10.1364/CLEO_SI.2016.STu4G.8](https://doi.org/10.1364/CLEO_SI.2016.STu4G.8)
- [14] William Shieh, Chuan Bowen Sun, and Honglin Ji, "Carrier-assisted differential detection," *Light: Science & Applications*, vol. 9, no. 1, pp. 1–9, 2020. DOI: [10.1038/s41377-020-0253-8](https://doi.org/10.1038/s41377-020-0253-8)